The Influence of Substituents on Cation−π Interactions. 4. Absolute Binding Energies of Alkali Metal Cation−Phenol Complexes Determined by Threshold Collision-Induced Dissociation and Theoretical Studies[†,‡]

R. Amunugama and M. T. Rodgers*

Department of Chemistry, Wayne State University, Detroit, Michigan 48202

Received: May 9, 2002; In Final Form: July 2, 2002

The kinetic energy dependence of the collision-induced dissociation of $M^+(C_6H_5OH)$ and $M^+(C_6H_5OH)_2$ with Xe is studied using guided ion beam mass spectrometry. M^+ includes the following alkali metal cations: Li^+, Na^+, K^+, Rb^+, and Cs^+. The primary dissociation channel observed in all complexes is endothermic loss of an intact phenol ligand. Sequential dissociation of a second phenol ligand is observed at elevated energies in the bis-complexes. The cross section thresholds for the primary dissociation channel are interpreted to yield 0 and 298 K bond dissociation energies for $(C_6H_5OH)_{x-1}M^+-C_6H_5OH$, $x = 1-2$, after accounting for the effects of multiple ion−neutral collisions, the kinetic and internal energies of the reactants, and dissociation lifetimes. Ab initio and density functional theory calculations at the MP2(full)/6-311+G(2d,2p)//B3LYP/6-31G* level of theory are used to determine the structures, molecular constants, and theoretical binding energies of these complexes. The agreement between theory and experiment is good when full electron correlation is included, except for the $Li^+(C_6H_5OH)$ complex, and somewhat less satisfactory when effective core potentials are used. The experimental value for $Na^+-C_6H_5OH$ bond energy determined here is within experimental error of the value previously reported. The trends in $M^+(C_6H_5OH)_x$ binding energies are explained in terms of varying magnitudes of electrostatic interactions and ligand−ligand repulsion in the complexes. Comparisons are also made with the other cation−π complexes to benzene to examine the influence of the hydroxyl substituent on the binding, and the factors that control the strength of cation−π interactions.

Introduction

The phenol molecule is a good model for the side chain of the naturally occurring aromatic amino acid, tyrosine (Tyr). An interesting feature of both phenol and the side chain of tyrosine is the presence of multiple cation-binding sites, the π-cloud above the aromatic ring, and the lone pair of electrons on the hydroxyl oxygen atom. Because tyrosine is known to participate in a variety of important biological processes, there have been several experimental and theoretical studies reported in the literature involving phenol and/or tyrosine. The role of tyrosine in these processes is believed to involve cation−π interactions.[1,2] Cation−π interactions are noncovalent interactions that are believed to play important roles in protein structural organization[1−7] and the functioning of ionic channels in membranes.[8,9] In their study, Heginbotham and MacKinnon observed altered selectivity for K^+ over Na^+ when the crucial pore tyrosine residue in a voltage-gated channel was mutated to valine.[10] Later studies from Gaber and co-workers[11] on inward-rectifying channels suggest an absolute requirement for an aromatic residue at this site to achieve the highly selective behavior of the natural K^+ channels. Additional mutagenesis studies on another feature of a voltage-gated K^+ channel, blocked by organic cations such as tetraethylammonium (TEA), established that specific Tyr residues play a crucial role in the functioning of this channel. A site-directed mutagenesis study identified the 449 Tyr residue located near the mouth of the pore to be crucial to TEA binding.[12−15] In fact the family of high TEA affinity K^+ channels all possess a Tyr residue at this crucial site. In contrast, ion channels with low TEA affinity (e.g., *Shaker*) have a nonaromatic residue such as threonine at this position. In addition, it is reported that high-affinity binding to TEA can be brought about in *Shaker* by mutation of this residue to Tyr.[12,13] Further, sequence comparison between the high- and low-affinity toxin-binding Na^+ channels demonstrates the importance of aromatic residues at specific locations. The cardiac Na^+ channels are less sensitive to Guanidinium toxins tetrodotoxin (TTX) than the brain or skeletal muscle Na^+ channels. Among these channels, only two residues are distinct, a phenylalanine (Phe)/cysteine (Cys) pair in the pore region. When this Cys residue in cardiac channels was mutated to Tyr or Phe, the TTX-blocking efficiency increased by 730-fold.[16] It was suggested that the aromatic residue binds to the TTX in these channels through a cation−π interaction with an arginine (Arg) residue of the toxin. These studies illustrate the importance of cation−π interactions between aromatic amino acid residues and cations, and in particular the role played by Tyr residues, to the structure and functioning of cation transport proteins. As suggested by these studies, cation−π interactions involving Na^+ and K^+ are the most biologically relevant.[17] However, systems involving the larger alkali metal cations (e.g., Cs^+) have also been reported in the literature.[18] Thus, the understanding cation−π interactions involving alkali metal cations from a fundamental perspective as well as the detailed role that they play in biological systems is of paramount importance.

To gain a better understanding of the interaction of alkali metal cations with large biological molecules, knowledge of the structure and energetics of binding to smaller model systems

[†] Part of the special issue "Jack Beauchamp Festschrift".

[‡] In honor of J. L. Beauchamp on the occasion of his 60th birthday, in thanks for his numerous contributions to gas-phase ion chemistry, and in appreciation for his mentoring and friendship.

* To whom correspondence should be addressed.

10.1021/jp0211584 CCC: $22.00
Published on Web 09/11/2002

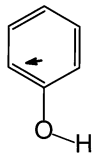

Figure 1. Structure of the phenol molecule. The properly scaled dipole moment in Debye is shown as an arrow. Values listed are taken from experiment[39] and theoretical calculations performed here (in parentheses). The estimated polarizability is also shown.[40]

is required. Furthermore, characterizing these interactions in the gas phase is an important and essential part of building a database of information concerning the nature and strength of cation−π interactions and the influence of the local environment on such interactions. Many model systems in which the neutral ligand binds to the cation through its π electrons,[19−28] as well as the aromatic amino acids[29,30] have been experimentally studied in the gas phase. Among the model systems examined, benzene,[19−24] pyrrole,[25,26] and their derivatives such as toluene,[28] phenol,[23,36] indole,[27] fluorobenzene,[31] and aniline[32] are of particular interest. These model systems constitute the simplest groups of larger aromatic ligands that could mimic the binding properties of π-donating ligands believed to participate in cation−π interactions operative in biological systems. High-level theoretical calculations have also been performed for several of the systems above at various levels of theory.[1,25−28,33,34]

To understand the influence of substituents on cation−π interactions, we set out to determine the absolute binding energies of alkali metal cations to several substituted benzene ligands. In these studies, we previously examined the influence of the methyl,[28] fluoro,[31] and amino[32] substituents. In the present study, we examined the influence of a hydroxyl substituent by examining cation−π interactions between the alkali metal cations (Li^+, Na^+, K^+, Rb^+, and Cs^+) and phenol. Several experimental and theoretical studies that examined the interactions of Na^+[23,27,35−37] K^+,[27] Mg^+,[27] Al^+,[27] Cr^+,[27,38] Fe^+,[27,38] and Co^+,[38] with phenol have previously been reported. However, experimental studies of cation−π interactions between phenol and the other the alkali metal cations have not been reported in the literature. The structure of phenol along with its measured[39] and calculated dipole moments (determined here) and estimated polarizability[40] are shown in Figure 1. The kinetic energy-dependent cross sections for the primary collision-induced dissociation (CID) process observed in each system are analyzed by methods developed previously.[41] The analysis explicitly includes the effects of the internal and translational energy distributions of the reactants, multiple ion−neutral collisions, and the lifetime for dissociation. We derive $(C_6H_5OH)_{x-1}M^+$-C_6H_5OH, $x = 1-2$, bond dissociation energies (BDEs) for all of the complexes and compare these results with previous experimental measurements and with ab initio and density functional calculations performed here and in the literature.[23,27,35,37] Comparisons are also made with the analogous benzene,[24] toluene,[28] fluorobenzene,[31] and aniline[32] systems studied previously to compare the influence that each of these substituents has on the binding and the factors that control the strength of cation−π interactions.

Experimental Section

General Procedures. Cross sections for collision-induced dissociation of $M^+(C_6H_5OH)_x$ complexes, where $x = 1-2$, and $M^+ = Li^+$, Na^+, K^+, Rb^+, and Cs^+ are measured with a guided ion beam mass spectrometer that has been described in detail previously.[42] The $M^+(C_6H_5OH)_x$ complexes are generated in a flow tube ion source by condensation of the alkali metal cation and neutral phenol molecule(s). These complexes are collisionally stabilized and thermalized by $\sim 10^5$ collisions with the He and Ar bath gases such that the internal energies of the ions emanating from the source region are well described by a Maxwell−Boltzmann distribution at room temperature.[42] The ions are extracted from the source, accelerated, and focused into a magnetic sector momentum analyzer for reactant ion mass selection. Mass-selected ions are decelerated to a desired kinetic energy and focused into an octopole ion guide, which acts as an efficient ion trap in the radial direction.[43] The octopole passes through a static gas cell containing Xe at low pressures (0.05−0.20 mTorr), to ensure that multiple ion−neutral collisions are improbable. The trapping field of the octopole efficiently focuses scattered reactant and product ions. These ions drift to the end of the octopole where they are focused into a quadrupole mass filter for mass analysis and subsequently detected with a secondary electron scintillation detector and standard pulse-counting techniques.

Ion intensities are converted to absolute cross sections using a Beer's law analysis.[44] Absolute uncertainties in cross section magnitudes are estimated to be ±20%, which are largely the result of errors in the pressure measurement and the length of the interaction region. Relative uncertainties are approximately ±5%. The cross sections for Li^+ products were more scattered and showed more variations in magnitude than is typical for heavier ions because the radio frequency used for the octopole does not trap light masses with high efficiency. Therefore, absolute magnitudes of the cross sections for production of Li^+ are probably accurate to ±50%.

Ion kinetic energies in the laboratory frame, E_{lab}, are converted to energies in the center of mass (CM) frame. All energies reported below are in the CM frame unless otherwise noted. The absolute zero and distribution of the ion kinetic energies are determined using the octopole ion guide as a retarding potential analyzer.[44] For the experiments performed here, the distribution of ion kinetic energies is nearly Gaussian with a full width at half-maximum (fwhm) typically between 0.2 and 0.4 eV (lab). The uncertainty in the absolute energy scale is ±0.05 eV (lab).

Because multiple collisions can influence the shape of CID cross sections and the threshold regions are most sensitive to these effects, we have performed pressure-dependent studies of all cross sections examined here. Data free from pressure effects are obtained by extrapolating to zero reactant pressure, as described previously.[45] Thus, results reported below are due to single bimolecular encounters.

Thermochemical Analysis. The threshold regions of the primary CID cross sections are modeled using eq 1,

$$\sigma(E) = \sigma_0 \sum_i g_i (E + E_i - E_0)^n / E \qquad (1)$$

where σ_0 is an energy-independent scaling factor, E is the relative translational energy of the reactants, E_0 is the threshold for reaction of the ground electronic and ro-vibrational state, and n is an adjustable parameter. The summation is over the ro-vibrational states of the reactant ions, i, where E_i is the excitation energy of each ro-vibrational state and g_i is the population of those states ($\Sigma g_i = 1$).

The density of ro-vibrational states is evaluated using the Beyer−Swinehart algorithm,[46] and the relative populations, g_i are calculated by a Maxwell−Boltzmann distribution at the 298

K temperature appropriate for the reactants. The vibrational frequencies of the reactant complexes are determined from density functional theory calculations as discussed in the Theoretical Calculations section. The average vibrational energy at 298 K of the $M^+(C_6H_5OH)_x$ complexes is given in the Supporting Information in Table S1. To account for the inaccuracies in the calculated frequencies, we have increased and decreased the scaled calculated frequencies by 10% for the $M^+(C_6H_5OH)_x$ complexes to Li^+, Na^+, and K^+. This scaling procedure encompasses the range of scale factors needed to bring calculated frequencies into agreement with experimentally determined frequencies as found by Pople et al.[47] For the $M^+(C_6H_5OH)_x$ complexes with Rb^+ and Cs^+, 20% variations were applied. The corresponding change in the average vibrational energy is taken to be an estimate of one standard deviation of the uncertainty in the vibrational energy (Table S1).

We also include statistical theories for unimolecular dissociation, specifically Rice−Ramsperger−Kassel−Marcus (RRKM) theory, in eq 1[41,48] to account for the possibility that collisionally activated ions may not have undergone dissociation before arriving at the detector ($\sim 10^{-4}$ s). The ro-vibrational frequencies appropriate for the energized molecules, and the transition states (TSs) leading to dissociation, are given in Tables S1 and S2. In our analysis, we assume that the TSs are loose and product-like because the interaction between the alkali metal cation and the phenol ligand(s) is largely electrostatic. The most appropriate model for the TS of such electrostatically bound complexes is a loose phase space limit (PSL) model located at the centrifugal barrier for the interaction of $M^+(C_6H_5OH)_{x-1}$ with C_6H_5OH as described in detail elsewhere.[41] The TS vibrations appropriate for this model are the frequencies of the products, which are also found in Table S1. The transitional frequencies, those that become rotations of the completely dissociated products, are treated as rotors. The transitional mode rotors and the one-dimensional external rotor of the TS are simply the rotational constants of the molecular product(s) formed in the CID reaction.[41] These are listed in Table S2. The two-dimensional (2-D) external rotational constant of the TS is determined by assuming that the TS occurs at the centrifugal barrier for interaction of $M^+(C_6H_5OH)_{x-1}$ with the neutral C_6H_5OH molecule, treated variationally as outlined elsewhere.[41] The 2-D external rotations are treated adiabatically but with centrifugal effects included using a statistical distribution with explicit summation over the possible values of the rotational quantum number.[41]

The model represented by eq 1 is expected to be appropriate for translationally driven reactions[49] and has been found to reproduce CID cross sections well. The model is convoluted with the kinetic energy distributions of both reactants, and a nonlinear least-squares analysis of the data is performed to give optimized values for the parameters σ_0, E_0, and n. The error associated with the determination of the threshold energy, E_0, is estimated from the range of threshold values determined for different zero-pressure extrapolated data sets, variations associated with uncertainties in the vibrational frequencies, and the error in the absolute energy scale, 0.05 eV (lab). For analyses that include the unimolecular lifetime analysis, the uncertainties in the reported E_0 values also include the effects of increasing and decreasing the time assumed available for dissociation by a factor of 2.

Equation 1 explicitly includes the internal energy of the ion, E_i. All energy available is treated statistically because the energy of the reactants is redistributed throughout the ion in the collision. Because the CID processes examined here correspond to simple noncovalent bond fission reactions, the E_0 values determined by analysis using eq 1 can be equated to 0 K bond energies.[50,51]

Theoretical Calculations. To obtain model structures, vibrational frequencies, rotational constants, and energetics for the neutral C_6H_5OH ligand and for the $M^+(C_6H_5OH)_x$ complexes, ab initio and density functional theory calculations were performed using *Gaussian 98*.[52] Geometry optimizations were performed at B3LYP/6-31G* level[53,54] for the $M^+(C_6H_5OH)_x$ complexes where $M^+ = Li^+$, Na^+, and K^+. For complexes to Rb^+ and Cs^+, geometry optimizations were performed using a hybrid basis set in which the effective core potentials (ECP) and valence basis sets of Hay and Wadt were used to describe the metal cation,[55] whereas 6-31G* basis sets were used for C, O, and H atoms. As suggested by Glendening et al.,[56] a single polarization (d) function was added to the Hay−Wadt valence basis set for Rb and Cs, with exponents of 0.24 and 0.19, respectively.

Vibrational analyses of the geometry-optimized structures were performed to determine the vibrational frequencies for the neutral C_6H_5OH ligand and the $M^+(C_6H_5OH)_x$ complexes for $M^+ = Li^+$, Na^+, and K^+. The vibrational frequencies for the $M^+(C_6H_5OH)_x$ complexes where $M^+ = Rb^+$ and Cs^+ were estimated by scaling the calculated frequencies for the analogous $K^+(C_6H_5OH)_x$ complexes using a procedure described in detail previously.[57] When used to model data or calculate thermal energy corrections, the calculated vibrational frequencies were scaled by a factor of 0.9804.[58] The vibrational frequencies and rotational constants of C_6H_5OH and all ten $M^+(C_6H_5OH)_x$ complexes are listed in the Supporting Information in Tables S1 and S2, respectively. Single point energy calculations were performed at the MP2(full)/6-311+G(2d,2p) level using the B3LYP/6-31G* and B3LYP/Hybrid (6-31G*, Hay−Wadt) optimized geometries. To obtain accurate BDEs, zero point energy (ZPE) corrections were applied and basis set superposition errors (BSSE) were subtracted from the computed dissociation energies in the full counterpoise correction.[59,60] The ZPE corrections are small and decrease with increasing size of the alkali metal cation. The BSSE corrections are somewhat larger, but also decrease with increasing size of the metal cation. Calculations of the corresponding σ-binding complexes were also performed for the $M^+(C_6H_5OH)$ complexes. In these complexes, the ZPE and BSSE corrections are somewhat smaller than for the cation−π complexes, as expected, because the cation interacts with a single site and therefore exerts a lesser influence on the ligand.

Results

Cross Sections for Collision-Induced Dissociation. Experimental cross sections were obtained for the interaction of Xe with ten $M^+(C_6H_5OH)_x$ complexes, where $M^+ = Li^+$, Na^+, K^+, Rb^+, and Cs^+, and $x = 1$ and 2. Figure 2 shows representative data for the $Na^+(C_6H_5OH)_x$, $x = 1$ and 2 complexes. The other $M^+(C_6H_5OH)_x$ complexes exhibit similar behavior and are included in the Supporting Information as Figure S1. The sequential loss of intact phenol molecules and ligand exchange with Xe are the only processes observed in these systems over the collision energy range studied, typically 0 to >5 eV. The dominant process observed for all of these complexes is the loss of a single intact phenol molecule in the CID reaction 2.

$$M^+(C_6H_5OH)_x + Xe \rightarrow M^+(C_6H_5OH)_{x-1} + C_6H_5OH + Xe \quad (2)$$

TABLE 1: Fitting Parameters of Equation 1, Threshold Dissociation Energies at 0 K, and Entropies of Activation at 1000 K[a]

reactant complex	σ_0[b]	n[b]	E_0[c] (eV)	E_0(PSL) (eV)	kinetic shift (eV)	$\Delta S^{\dagger}$ (PSL) (J mol^{-1} K^{-1})
$Li^+(C_6H_5OH)$	1.1 (0.2)	1.7 (0.1)	2.01 (0.22)	1.85 (0.17)	0.16	49 (3)
$Na^+(C_6H_5OH)$	13.3 (0.4)	1.4 (0.1)	1.06 (0.04)	1.06 (0.04)	0.00	40 (2)
$Na^+(C_6H_5OH)$[d]	14.9 (1.1)	1.0 (0.1)	1.02 (0.04)	1.02 (0.04)	0.00	47 (2)
$K^+(C_6H_5OH)$	27.9 (2.7)	1.1 (0.1)	0.77 (0.03)	0.77 (0.03)	0.00	35 (3)
$Rb^+(C_6H_5OH)$	18.7 (0.3)	1.0 (0.1)	0.71 (0.05)	0.71 (0.05)	0.00	43 (5)
$Cs^+(C_6H_5OH)$	21.9 (1.1)	1.2 (0.1)	0.67 (0.05)	0.67 (0.05)	0.00	47 (5)
$Li^+(C_6H_5OH)_2$	48.8 (2.3)	1.3 (0.1)	1.32 (0.05)	1.19 (0.03)	0.13	47 (5)
$Na^+(C_6H_5OH)_2$	75.7 (3.2)	1.3 (0.1)	0.88 (0.05)	0.85 (0.03)	0.03	37 (5)
$K^+(C_6H_5OH)_2$	70.4 (1.5)	1.0 (0.1)	0.73 (0.03)	0.70 (0.03)	0.03	9 (5)
$Rb^+(C_6H_5OH)_2$	26.2 (2.3)	1.3 (0.1)	0.69 (0.06)	0.66 (0.04)	0.03	11 (5)
$Cs^+(C_6H_5OH)_2$	30.4 (1.1)	1.3 (0.1)	0.65 (0.08)	0.63 (0.04)	0.02	13 (9)

[a] Uncertainties are listed in parentheses. [b] Average values for loose PSL transition state. [c] No RRKM analysis. [d] Previous threshold collision-induced dissociation work by Armentrout and Rodgers.[23]

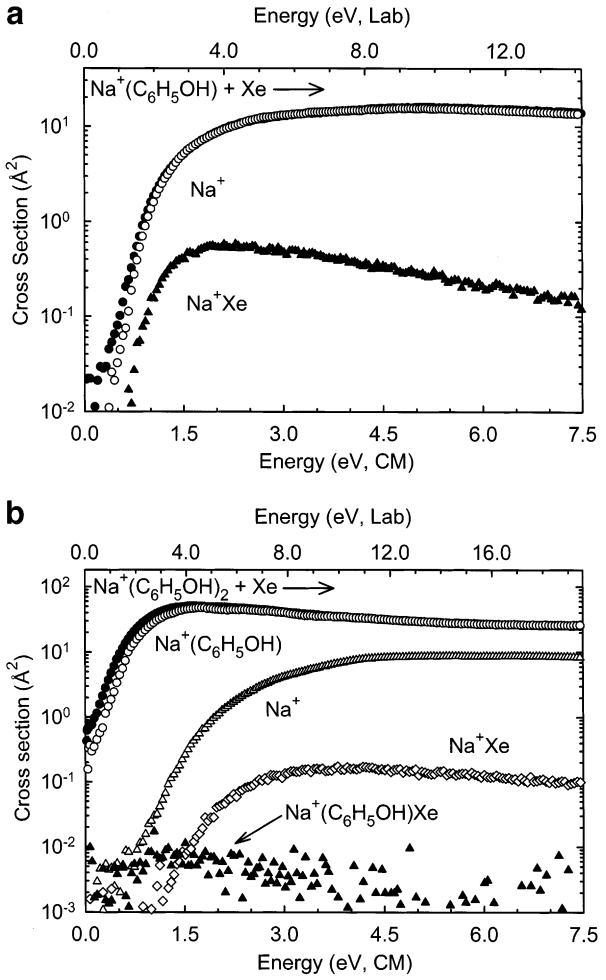

Figure 2. Cross sections for collision-induced dissociation of $Na^+(C_6H_5OH)_x$, $x = 1$ and 2 (parts a and b, respectively), with Xe as a function of kinetic energy in the center-of-mass frame (lower *x*-axis) and the laboratory frame (upper *x*-axis). Data are shown for a Xe pressure of ~0.2 and ~0.1 mTorr, for the $x = 1$ and 2 complexes, respectively. Primary and secondary product cross sections are shown as ● and △, respectively. Primary and secondary ligand exchange product cross sections are shown as ▲ and ◇, respectively. Data are also shown for the primary product cross section, extrapolated to zero pressure of Xe as ○.

In the $M^+(C_6H_5OH)$ complexes, the thresholds for reaction 2 decrease and the maximum cross sections increase as the size of the alkali metal cation increases, behavior consistent with electrostatic binding. The complexes to Rb^+ and Cs^+ deviate somewhat from these simple trends in that they exhibit cross section maxima that are intermediate between that observed for the Na^+ and K^+ complexes. Similar behavior is observed in the $M^+(C_6H_5OH)_2$ complexes, where the thresholds for reaction 2 decrease and the maximum cross sections increase with increasing size of the alkali metal cation. The Rb^+ and Cs^+ systems again deviate from these simple trends, exhibiting cross sections that are smaller than for all of the other alkali metal cations. The thresholds for reaction 2 decrease and the cross section maxima roughly double from the mono- to the corresponding bis-complex; behavior that is again indicative of the electrostatic nature of the binding in these complexes. At elevated energies, dissociation of a second C_6H_5OH ligand is observed in the $M^+(C_6H_5OH)_2$ complexes. The cross section for the primary CID product declines as the secondary CID product is formed indicating that this product is formed sequentially from the primary CID product.

In addition to the CID processes, ligand-exchange reactions are also observed. The apparent thresholds for the ligand-exchange processes in the $M^+(C_6H_5OH)_x$ complexes decrease regularly as the size of the cation increases and are smaller for the mono-complexes than the bis-complexes. The cross section magnitudes of the ligand exchange products are quite small. The primary and secondary ligand exchange products are approximately 3 and 2 orders of magnitude smaller than the primary CID product, respectively.

Threshold Analysis. The model of eq 1 was used to analyze the thresholds for reactions 2 in ten $M^+(C_6H_5OH)_x$ systems. The results of these analyses are given in Table 1 for all ten $M^+(C_6H_5OH)_x$ complexes. Representative fits using eq 1 for the $Na^+(C_6H_5OH)_x$ complexes are shown in Figure 3. A comparable set of figures for the other $M^+(C_6H_5OH)_x$ complexes are available in the Supporting Information as Figure S2. Experimental cross sections for the primary dissociation processes of the $M^+(C_6H_5OH)_x$ complexes are accurately reproduced using a loose PSL TS model.[41] This model has been shown to provide the most accurate determination of kinetic shifts for CID of electrostatically bound metal−ligand complexes.[41] The data are accurately reproduced across energy ranges exceeding 1 eV and across cross section magnitudes of at least a factor of 100 for all complexes except $Rb^+(C_6H_5OH)_2$ and $Cs^+(C_6H_5OH)_2$, because the primary cross sections observed for these complexes are already nonzero at 0 eV. Threshold values, E_0, obtained from analyses of the data without consideration of lifetime effects are also included in Table 1. The kinetic shifts, the differences between these values and those obtained when lifetime effects are included, E_0(PSL), are also given in Table 1. Although the $M^+(C_6H_5OH)$ and $M^+(C_6H_5OH)_2$ complexes have 36 and 75 vibrational modes, respectively, the kinetic shifts observed for these systems are quite small. Of the mono-ligated complexes, only $Li^+(C_6H_5OH)$, the most

TABLE 2: Geometrical Parameters of B3LYP/6-31G* Optimized Structures of the $M^+(C_6H_5OH)_x$ Complexes

complex	M−C (Å)	M−centroid (Å)[a]	M^+−O (Å)	C−C (Å)	C−H (Å)	C−H OOP angle (deg)[b]	C−O H (Å)	O−H (Å)
C_6H_5OH				1.400	1.090	0.000	1.369	0.970
$Li^+(C_6H_5OH)$	2.359	1.881		1.407	1.090	0.817	1.343	0.973
$Li^+(C_6H_5OH)$[d]			1.855	1.397	1.090	1.861	1.414	0.973
$Na^+(C_6H_5OH)$	2.767	2.387		1.405	1.090	0.705	1.351	0.972
$Na^+(C_6H_5OH)$[d]			2.226	1.400	1.090	1.800	1.405	0.972
$K^+(C_6H_5OH)$	3.198	2.876		1.403	1.090	0.618	1.357	0.972
$K^+(C_6H_5OH)$[d]			2.635	1.400	1.090	1.430	1.400	0.972
$Rb^+(C_6H_5OH)$[c]	3.477	3.183		1.402	1.090	0.391	1.360	0.971
$Rb^+(C_6H_5OH)$[c,d]			2.887	1.400	1.090	1.306	1.395	0.971
$Cs^+(C_6H_5OH)$[c]	3.733	3.459		1.401	1.090	0.310	1.362	0.971
$Cs^+(C_6H_5OH)$[c,d]			3.128	1.400	1.090	1.127	1.393	0.971
$Li^+(C_6H_5OH)_2$	2.480	2.059		1.404	1.090	0.578	1.350	0.972
$Na^+(C_6H_5OH)_2$	2.829	2.456		1.403	1.090	0.554	1.354	0.972
$K^+(C_6H_5OH)_2$	3.239	2.922		1.402	1.090	0.494	1.359	0.971
$Rb^+(C_6H_5OH)_2$[c]	3.507	3.215		1.401	1.090	0.342	1.361	0.971
$Cs^+(C_6H_5OH)_2$[c]	3.766	3.494		1.400	1.090	0.266	1.363	0.971

[a] The metal ring-centroid distance is defined as the distance from the metal atom to the central point within the aromatic ring of phenol that is in the plane of the carbon atoms. [b] Out-of-plane angle. [c] The Hay−Wadt ECP/valence basis set was used for the metal ion, as described in the text, and the 6-31G* basis set for C, O, and H. [d] Complexes in which the alkali metal ion interacts with the hydroxyl substituent.

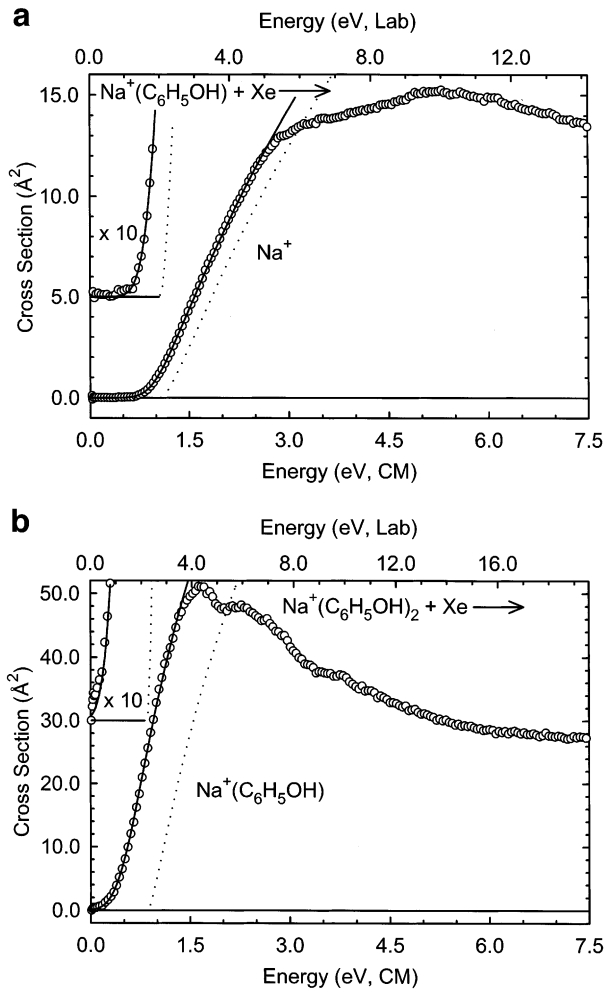

Figure 3. Zero-pressure extrapolated cross sections for the primary collision-induced dissociation product of the $Na^+(C_6H_5OH)_x$ complexes, $x = 1$ and 2 (parts a and b, respectively), with Xe in the threshold region as a function of kinetic energy in the center-of-mass frame (lower *x*-axis) and the laboratory frame (upper *x*-axis). Solid lines show the best fits to the data using the model of eq 1 convoluted over the neutral and ion kinetic and internal energy distributions. Dashed lines show the model cross sections in the absence of experimental kinetic energy broadening for reactants with an internal energy of 0 K.

strongly bound complex, exhibits a kinetic shift, 0.16 eV. All of the bis-complexes exhibit small kinetic shifts that vary from 0.02 to 0.13 eV. The kinetic shifts decrease with increasing size of the cation, from Li^+ to Cs^+. This is easily understood because the observed kinetic shift should directly correlate with the density of states of the complex at threshold, which depends on the measured BDE, as observed (Table 1).

The entropy of activation, $\Delta S^\dagger$, is a measure of the looseness of the TS. It is also a reflection of the complexity of the system because it is largely determined by the molecular parameters used to model the energized molecule and the TS, but also depends on the threshold energy. The $\Delta S^\dagger$(PSL) values at 1000 K are listed in Table 1 and vary between 9 and 49 J K^{-1} mol^{-1}. These entropies of activation compare favorably with an expanding range of noncovalently bound metal−ligand complexes previously measured in our laboratory and with those collected by Lifshitz for simple bond cleavage reactions of ions.[61]

Theoretical Results. Theoretical structures for neutral phenol and for the mono- and bis-ligated complexes of phenol with Li^+, Na^+, K^+, Rb^+, and Cs^+ were calculated as described above. Details of the geometry-optimized structures for each of these species are given in Table 2. The cation−π complexes of $Na^+(C_6H_5OH)$ and $Na^+(C_6H_5OH)_2$ are shown in Figure 4. The metal cation binds to the π cloud of the aromatic ring of the phenol molecule, a cation−π interaction. The distortion of the phenol molecule that occurs upon complexation to the alkali metal cation is minor. The change in geometry is largest for Li^+ and decreases with increasing size of the metal cation. The M^+−C and M^+−ring-centroid distances[62] are found to increase as the size of the metal cation increases for both the mono- and bis-complexes. These distances are also found to increase on going from the mono- to the corresponding bis-complex. The computed Na^+−C distance in the $Na^+(C_6H_5OH)$ π complex of 2.767 Å is 0.006 Å shorter than that previously found by Hoyau et al.[37] The M^+−ring-centroid distance of the $Na^+(C_6H_5OH)$ π complex, 2.387 Å, found here agrees quite well with that calculated by Ryzov and Dunbar.[27]

As seen in Figure 4, the cation−π complex of $Na^+(C_6H_5OH)$ has the Na^+ ion interacting with the π cloud of the aromatic ring. However, it is also possible that the metal cation might interact with the lone pairs of electrons on the oxygen atom through a σ-type interaction. Stable σ-binding conformers were also calculated for the Li^+, Na^+, K^+, Rb^+, and Cs^+ complexes to phenol. The optimized structure of the σ-binding conformer of $Na^+(C_6H_5OH)$ is shown in Figure 5. In these σ-binding

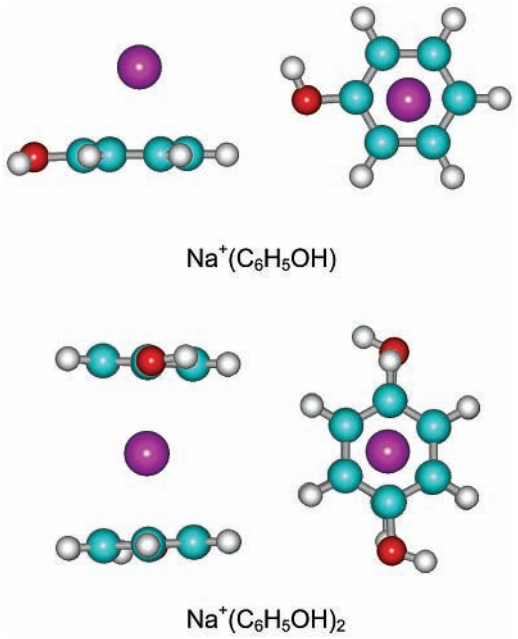

Figure 4. B3LYP/6-31G* optimized geometries of the cation−π complexes of $Na^+(C_6H_5OH)_x$, where $x = 1-2$. Two views of each optimized structure are shown.

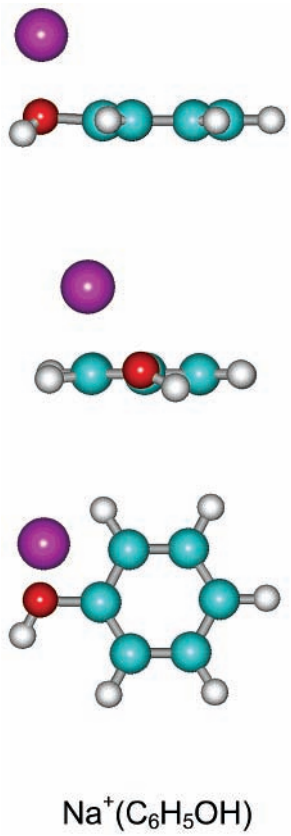

Figure 5. B3LYP/6-31G* optimized geometry of the conformer of $Na^+(C_6H_5OH)_x$ in which Na^+ binds to the hydroxy substituent. Three views of the optimized structure are shown.

complexes, the metal cation lies above the plane of the aromatic ring and is located between the two lone pairs of electrons on the oxygen atom of the phenol ligand. At the MP2(full)/6-311+G(2d,2p) level of theory, the σ-binding conformers of Li^+ and K^+ are found to be 7.5 and 1.5 kJ/mol less stable than the corresponding cation−π complexes. In contrast, the σ-binding conformers of Na^+ and Rb^+ are found to be 0.6 and 1.5 kJ/mol more stable than the corresponding cation−π complexes. The $Cs^+(C_6H_5OH)$ exhibits intermediate behavior in that the π and σ complexes are found to be degenerate at this level of theory. The greater stability of the σ-binding conformer of the $Na^+(C_6H_5OH)$ complex was previously suggested by Hoyau et al.[37] and Ryzhov and Dunbar.[27] Calculations performed in their earlier work found the σ-binding conformer is more stable by 0.4 and 2.0 kJ/mol, respectively, than the $Na^+(C_6H_5OH)$ cation−π complex. When ZPE and BSSE corrections are not included in the calculations performed here, the cation−π complexes are more stable than the corresponding σ-binding conformers for all of the alkali metal cations by 13.1, 2.8, 3.3, 0.4, and 0.7 kJ/mol for Li^+, Na^+, K^+, Rb^+ and Cs^+, respectively. The similar energies of the cation−π and σ-binding conformers calculated for these systems suggests that the ion beams generated in our experiments are likely composed of a mixture of both species. Because the technique used here to determine the BDEs of these complexes is a threshold technique, our results should correlate with the less strongly bound conformer present in reasonable abundance. The population of the σ-binding conformer of the $Li^+(C_6H_5OH)$ complex should be quite small and is therefore unlikely to influence the threshold determination.

As also seen in Figure 4, the lowest energy structure for the $Na^+(C_6H_5OH)_2$ complex has the Na^+ ion interacting with the π clouds of the aromatic rings and has the hydroxyl substituents oriented anti to one another to minimize repulsive ligand−ligand interactions associated with the hydroxyl groups. The anti configuration was found to be the lowest energy structure for all of the $M^+(C_6H_5OH)_2$ complexes. To estimate the barrier to free rotation of the aromatic ring in the bis-complexes, optimizations were also performed for $Li^+(C_6H_5OH)_2$ with the hydroxyl groups syn, "ortho", and "meta" to one another. These complexes were found to be 4.2, 1.8, and 1.0 kJ/mol less stable than when oriented anti to one another (excluding BSSE corrections). Thus, the barrier to free rotation in the $Li^+(C_6H_5OH)_2$ complex is quite small and should be even smaller for the complexes to the other alkali metal cations because the phenol ligands are further apart. Therefore, at room temperature these complexes should have sufficient energy to interconvert freely (see Table S1).

As for the mono-complexes, the bis-complexes might also involve interaction of the alkali metal cation with the lone pairs of electrons on the oxygen atom through a σ-type interaction. In this case, two different conformations are possible, one in which one phenol ligand interacts through a cation−π interaction and the other phenol ligand through a σ-type interaction, and a second conformer in which both phenol ligands interact with the alkali metal cation through a σ-type interaction. To assess the relative stabilities of these alternate conformations, optimizations were also performed for $Li^+(C_6H_5OH)_2$ in these two conformations. At the MP2(full)/6-311+G(2d,2p) level of theory, these complexes were found to be 8.5 and 27.1 kJ/mol less stable than the corresponding complex in which both ligands bind through a cation−π interaction. This suggests that such conformers are unlikely to play a role in our experiments for Li^+. However, the σ- and π-binding mono-complexes are much closer in energy for the other alkali metal cations and are therefore probably of similar energy for the other alkali metal cations. Therefore, the bis-complexes to Na^+, K^+, Rb^+, and Cs^+ produced in our experiments are likely to be composed of a mixture of all three conformers.

Theoretical estimates for the $M^+(C_6H_5OH)_x$ BDEs were determined using the B3LYP/6-31G* geometries and single point energy calculations at MP2(full)/6-311+G(2d,2p) level

TABLE 3: Bond Dissociation Enthalpies of $M^+(C_6H_5OH)_x$ ($x = 1-2$ at 0 K in kJ/mol)

	experiment (TCID)		theory, X = OH				
complex	X = OH[a]	X = H[b]	D_e[c]	D_0[c,d]	$D_{0,BSSE}$[c,e]	D_e	$D_{0,BSSE}$
$Li^+(C_6H_5X)$	178.5 (16.1)	161.1 (13.5)	163.9	156.8	146.7		
			150.8[f]	146.6[f]	139.2[f]		
$Na^+(C_6H_5X)$	102.3 (3.4)	92.6 (5.8)	106.4	102.6	92.4		
	98.5 (3.4)[g]	88.3 (4.3)[g]					91.1[g]
						112.5[h]	
							91.4[i]
						104.2[j]	99.2[j]
			103.6[f]	101.4[f]	93.0[f]		91.8[f,i]
						104.2[f,j]	101.3[f,j]
$K^+(C_6H_5X)$	74.0 (3.4)	73.3 (3.8)	81.9	79.2	73.5		
			78.6[f]	77.0[f]	72.0[f]		
$Rb^+(C_6H_5X)$[k]	68.7 (4.4)	68.5 (3.8)	67.3	65.2	58.8		
			66.9[f]	65.4[f]	59.9[f]		
$Cs^+(C_6H_5X)$[k]	65.3 (4.9)	64.6 (4.8)	60.3	58.4	52.2		
			59.0[f]	57.7[f]	52.2[f]		
$Li^+(C_6H_5X)_2$	114.5 (3.2)	104.2 (6.8)	133.3	130.3	108.6		
$Na^+(C_6H_5X)_2$	81.6 (3.1)	80.0 (5.8)	97.7	94.6	78.5		
$K^+(C_6H_5X)_2$	68.4 (3.2)	67.5 (6.8)	75.6	73.4	63.2		
$Rb^+(C_6H_5X)_2$[k]	63.7 (4.4)	62.7 (7.7)	65.6	63.9	53.8		
$Cs^+(C_6H_5X)_2$[k]	60.4 (4.0)	58.8 (7.7)	56.8	55.8	47.0		

[a] Present results, Threshold collision-induced dissociation (TCID). Uncertainties are listed in parentheses. [b] Taken from Amicangelo and Armentrout, except as noted.[24] [c] Present work calculated at the MP2(full)/6-311+G(2d, 2p)//B3LYP/6-31G* level of theory. [d] Including zero point energy corrections with B3LYP/6-31G* frequencies scaled by 0.9804. [e] Also includes basis set superposition error corrections. [f] σ-binding conformer. [g] Armentrout and Rodgers calculated at the MP2(full)/6-311+G(2d,2p)//MP2(full)/6-31G* level of theory.[23] [h] Mecozzi et al. calculated at the HF/6-31G**//6-31G** level of theory.[35] [i] Hoyau et al. at calculated at MP2(full)/6-311+G(2d, 2p)//MP2(full)/6-31G* level of theory, 298 K values adjusted to 0 K.[37] [j] Ryzhov et al. calculated at B3LYP using a mixed valence basis set.[27] [k] The Hay−Wadt ECP/valence basis set was used for the metal ion, as described in the text, and the 6-31G* basis set and 6-311+G(2d, 2p) basis set were used for C, O, and H in geometry optimization and single point energy calculations, respectively.

of theory. In earlier work in which we measured and calculated the strength of cation−π interactions in $M^+(C_6H_5CH_3)_x$ complexes, we found that MP2(full)/6-311+G(2d,2p) theory was able to more accurately reproduce the experimentally measured BDEs than B3LYP/6-311+G(2d,2p) results.[28] The single point energy calculations performed here have therefore been limited to the former. These results are listed in Table 3 along with the experimental determinations performed here for phenol, and other theoretical results found in the literature.[23,27,35,37] Results shown in Table 3 also include ZPE and BSSE corrections.

Discussion

Trends in Experimental $M^+(C_6H_5OH)_x$ Bond Dissociation Energies. The 0 K experimental BDEs of the $M^+(C_6H_5OH)_x$ complexes are summarized in Table 3. The variation in the measured BDEs with the size of the alkali metal cation is shown in Figure 6 for both the mono- and bis-complexes. The $M^+-(C_6H_5OH)$ and $(C_6H_5OH)M^+-(C_6H_5OH)$ BDEs are found to decrease monotonically as the size of the metal cation increases from Li^+ to Cs^+. Similar trends were observed for the other aromatic ligands previously studied.[24,28,31,32] This is the expected trend for binding based primarily on electrostatic interactions.[1] The increasing size of the alkali metal cation[63] leads to larger metal−ligand bond distances (see Table 2), and the nonlinear distance dependencies of the electrostatic interactions fall off rapidly, as R^{-2} for ion−dipole, R^{-3} for the ion-quadrupole, and R^{-4} for ion-induced dipole interactions, resulting in the weaker binding to the larger alkali metal cations.

The BDEs of the $M^+(C_6H_5OH)_2$ complexes are smaller than the BDEs of the corresponding $M^+(C_6H_5OH)$ complexes in all cases. The decrease in the measured BDE on going from the mono- to bis-ligated system is largest for the Li^+, and decreases with increasing size of the alkali metal cation. The sequential BDE is found to decrease by 64.0, 20.7, 5.6, 5.0, and 4.9 kJ/mol for the Li^+, Na^+, K^+, Rb^+, and Cs^+ systems, respectively.

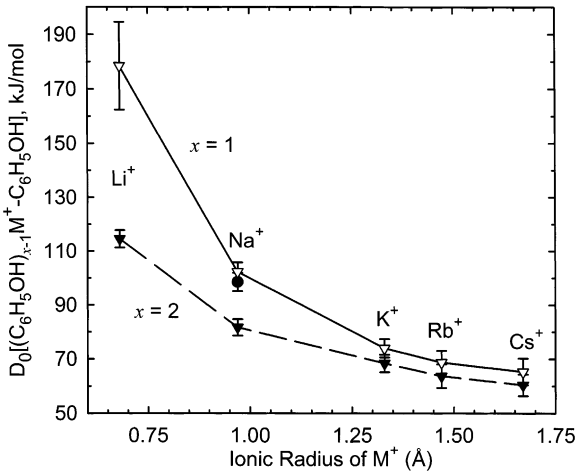

Figure 6. Bond dissociation energies at 0 K (in kJ/mol) of the $M^+(C_6H_5OH)_x$ complexes plotted versus the ionic radius of M^+. Data are shown for $x = 1$ and 2 as ▽ and ▼, respectively. Also shown is the value for $Na^+(C_6H_5OH)_x$ complex previously measured by Armentrout and Rodgers as ●.[23] All values are taken from Table 3.

Similar trends were observed for the other alkali metal cation−π complexes previously studied.[24,28,31,32] This behavior is the result of Coulombic and dipole−dipole repulsion between the phenol ligands. The distance between the aromatic rings is found to increase with increasing size of the metal cation, from ~4.12 Å in $Li^+(C_6H_5OH)_2$, to 6.98 Å in $Cs^+(C_6H_5OH)_2$ (Table 2, 2 × M^+−centroid distance). Clearly, the magnitude of the repulsive ligand−ligand interactions should decrease with increasing separation of the ligands. This should result in smaller differences in the BDEs for the mono- and bis-ligated complexes as the size of the alkali metal cation increases, as observed. The very small differences observed for the K^+, Rb^+, and Cs^+ complexes suggest that the distance between the phenol ligands

TABLE 4: Enthalpies and Free Energies Binding of $M^+(C_6H_5OH)_x$ $x = 1-2$ at 0 and 298 K in kJ/mol[a]

reactant complex	ΔH_0[b]	$\Delta H_{298} - \Delta H_0$[c]	ΔH_{298}	$T\Delta S_{298}$[c]	ΔG_{298}
$Li^+(C_6H_5OH)$	178.5 (16.1)	3.1 (2.8)	181.6 (16.3)	30.8 (6.4)	150.8 (17.5)
$Na^+(C_6H_5OH)$	102.3 (3.4)	1.3 (1.9)	103.6 (3.9)	28.6 (6.9)	75.0 (7.9)
$K^+(C_6H_5OH)$	74.0 (3.4)	0.6 (1.7)	74.6 (3.8)	26.8 (7.1)	47.8 (8.1)
$Rb^+(C_6H_5OH)$	69.6 (3.2)	0.6 (1.9)	70.2 (3.7)	28.4 (7.6)	41.8 (8.5)
$Cs^+(C_6H_5OH)$	65.6 (3.2)	0.6 (1.9)	66.2 (3.7)	29.1 (7.6)	31.1 (8.5)
$Li^+(C_6H_5OH)_2$	114.5 (3.2)	−3.0 (1.8)	111.5 (3.7)	36.8 (12.1)	74.7 (12.7)
$Na^+(C_6H_5OH)_2$	81.6 (3.1)	−2.9 (1.6)	78.7 (3.5)	34.2 (12.1)	44.5 (12.6)
$K^+(C_6H_5OH)_2$	68.4 (3.2)	−3.1 (1.4)	65.3 (3.5)	26.8 (12.2)	38.5 (12.7)
$Rb^+(C_6H_5OH)_2$	63.7 (3.3)	−3.1 (1.5)	60.6 (3.6)	29.1 (13.8)	31.4 (14.3)
$Cs^+(C_6H_5OH)_2$	60.8 (3.3)	−3.3 (1.3)	57.5 (3.6)	27.5 (13.7)	30.0 (14.1)

[a] Uncertainties are listed in parentheses. [b] Present experimental results (Table 3). [c] Density functional values from calculations at the B3LYP/6-31G* level of theory with frequencies scaled by 0.9804. The Hay−Wadt ECP/valence basis set was used for Rb^+ and Cs^+.

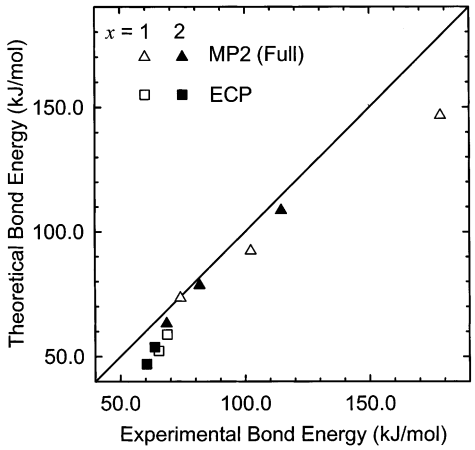

Figure 7. Theoretical versus experimental bond dissociation energies (in kJ/mol) at 0 K of the $M^+(C_6H_5OH)_x$ complexes. The diagonal line indicates the values for which the calculated and measured bond dissociation energies are equal. All values are taken from Table 3.

in these complexes is large enough that ligand−ligand repulsion is almost negligible.

Comparison of Theory and Experiment. The experimentally determined and theoretically calculated $M^+(C_6H_5OH)_x$ BDEs are listed in Table 3. The agreement between the experimental and theoretical BDEs determined at MP2(full)/6-311+G(2d,2p)//B3LYP/6-31G* level is illustrated in Figure 7. The theoretically determined BDEs are in good agreement with the measured BDEs for all complexes except $Li^+(C_6H_5OH)$. The mean absolute deviation (MAD) between the experimental and theoretical values for all 10 complexes is 10.3 ± 8.7 kJ/mol. This is somewhat larger than the average experimental error of 5.0 ± 3.9 kJ/mol. The MAD is larger for the mono-complexes, 13.0 ± 11.5 kJ/mol, than for the bis-complexes, 7.5 ± 4.1 kJ/mol. The agreement between the experimental and theoretical BDEs for the six $M^+(C_6H_5OH)_x$ complexes calculated including all electrons ($M^+ = Li^+$, Na^+, and K^+, $x = 1$ and 2) is reasonably good, with a MAD of 9.4 ± 11.4. The differences in these values are somewhat larger than the average experimental error in these values 5.4 ± 5.2 kJ/mol. Inspection of the data makes it clear than the Li^+ complex is the principal contributor to the MAD for these complexes. This poorer agreement may arise for two reasons. The first is the experimental difficulty in measuring cross sections for Li^+ as a result of the difficulty associated with efficient detection of this light mass. An alternative explanation is that theory may systematically underestimate the bond energies for Li^+ complexes as a result of the higher degree of covalency in the metal−ligand bond. This is shown by the calculated partial charge on M^+, which is 0.80*e* for $Li^+(C_6H_5OH)$ and varies between 0.90 and 0.99*e* for all of the other $M^+(C_6H_5OH)_x$ complexes at the MP2-(full)/6-31G(2d,2p) level. Therefore, higher levels of theory may be required to accurately describe the binding in this complex, a conclusion also drawn for Li^+ complexes with other ligands.[26,28,42] If the $Li^+(C_6H_5OH)$ value is not included, the MAD drops to 4.9 ± 3.5 kJ/mol, and the average experimental error also decreases to 3.3 ± 0.1 kJ/mol.

As pointed out earlier, as a good model for the side chain of Tyr, phenol has been examined in several previous studies. Many of these studies have been theoretical in nature and limited to Na^+ and/or K^+. In the earliest studies by Dougherty and coworkers,[35] calculations were performed at the HF/6-31G**//HF/6-31G** level of theory and did not include ZPE or BSSE corrections. At this level of theory, the binding energy of $Na^+(C_6H_5OH)$ is 112.5, 6.1 kJ/mol greater than the value calculated here. Hoyau et al.[37] calculated this BDE at MP2-(full)/6-311+G(2d,2p)//MP2/6-31G* level of theory and obtained 91.4 kJ/mol. Armentrout and Rodgers[23] calculated this BDE at MP2(full), B3LYP, B3P86, CBS, CBS-4M, and CBS-Q levels of theory using a 6-311+G(2d,2p) basis set for the single point energy calculations and obtained 91.1, 95.8, 95.3, 100.3, 96.3, and 101.9 kJ/mol, respectively. Ryzhov and Dunbar calculated this BDE at the B3LYP level of theory and obtained 99.2 kJ/mol. The higher level of theory used in the present work provides a BDE for $Na^+(C_6H_5OH)$ of 92.4 kJ/mol. The value measured here for $Na^+(C_6H_5OH)$, 102.3 ± 3.4 kJ/mol, is within experimental error, but 3.8 kJ/mol larger than that previously measured by Armentrout and Rodgers,[23] 98.5 ± 3.4 kJ/mol. The most accurate of these calculations is expected to be the CBS-Q complete basis set extrapolation, which is in excellent agreement with the values measured here (only 0.4 kJ/mol lower) and by Armentrout and Rodgers (only 3.4 kJ/mol higher).

The agreement between the experimental BDEs and the theoretical values calculated using the Hay−Wadt ECP/valence basis set for the Rb^+ and Cs^+ complexes is not as good. A MAD of 11.6 ± 1.9 kJ/mol is found. This is more than twice as large as the average experimental error in these values of 4.4 ± 0.4 kJ/mol. The deviations between the theoretical and experimental values are slightly larger for Cs^+ than Rb^+, and are larger for the mono-complexes than for the bis-complexes. As can be seen in Table 3 and Figure 7, the Hay−Wadt ECP/valence basis set results in calculated BDEs that are consistently lower than the experimentally measured values. Similar results were also found for the other cation−π complexes previously studied,[24,28,31,32] suggesting that the Hay−Wadt ECP/valence basis set results in calculated BDEs that are reasonably accurate, but systematically low.

Conversion from 0 to 298 K. The 0 K bond energies determined here are converted to 298 K bond enthalpies and free energies. The enthalpy and entropy conversions are

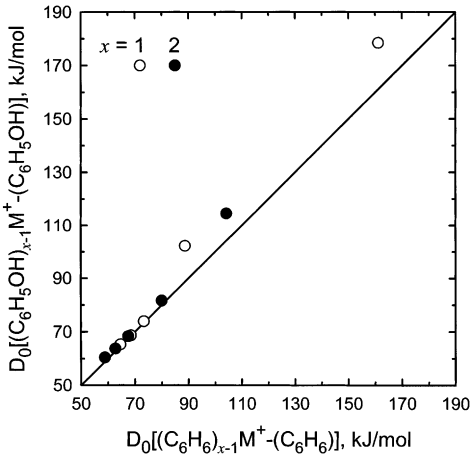

Figure 8. Experimental bond dissociation energies (in kJ/mol) at 0 K of the $(C_6H_5OH)_{x-1}M^+-(C_6H_5OH)$ versus $(C_6H_6)_{x-1}M^+-(C_6H_6)$, where $M^+ = Li^+$, Na^+, K^+, Rb^+, and K^+ and $x = 1$ (○) and 2 (●). Values for C_6H_6 are taken from Amicangelo and Armentrout.[24]

calculated using standard formulas (assuming harmonic oscillator and rigid rotor models) and the vibrational and rotational constants determined for the B3LYP/6-31G* optimized geometries. Table 4 lists 0 and 298 K enthalpies, free energies, and enthalpic and entropic corrections for all systems experimentally determined (from Table 1). The uncertainties in the enthalpic and entropic corrections are determined by 10% variation in the molecular constants for complexes to Li^+, Na^+, and K^+, and by 20% variation in the molecular constants for complexes to Rb^+ and Cs^+. Because the metal−ligand frequencies are very low and may not be adequately described by theory, the listed uncertainties also include contributions from scaling these frequencies up and down by a factor of 2. The latter provides a conservative estimate of the computational errors in these low-frequency modes and is the dominant source of error in the uncertainties listed.

Influence of the Hydroxyl Substituent. The effect of the hydroxyl substituent on the cation−π interaction can be examined by comparing the results obtained here for phenol, C_6H_5OH, to those obtained in earlier studies of benzene, C_6H_6,[24] toluene, $C_6H_5CH_3$,[28] fluorobenzene, C_6H_5F,[31] and aniline, $C_6H_5NH_2$.[32] In these earlier works, it was found that the influence of the substituent on the strength of the cation−π interaction could be explained by consideration of its influence of the quadrupole moment and polarizability of the aromatic ligand. In all of the cation−π complexes studied thus far, except those to aniline, the dipole moment of the aromatic ligand lies in the plane of the aromatic ring and thus an effective interaction of the alkali metal cation with the dipole moment is not possible.

As can be seen in Figure 8, the hydroxyl substituent results in a small increase in the strength of the cation−π interaction as compared with benzene. This enhancement in the cation−π interaction can be understood by examining the influence of the hydroxyl substituent on the dipole moment, quadrupole moment, and polarizability. Benzene possesses a center of symmetry and therefore has no dipole moment. Hydroxyl substitution breaks up the symmetry in the molecule and produces a dipole moment of 1.224 ± 0.008 D.[39] This measured value is somewhat lower than the value determined from our theoretical calculations, 1.40 D. However, as for toluene and fluorobenzene, the dipole moment of phenol lies in the plane of the aromatic ring, and therefore, an effective interaction of the alkali metal cation with the dipole moment is not possible in cation−π complexes to phenol. The delocalized π electron density above and below the plane of the aromatic ring results in a quadrupole moment for benzene of −8.69 DÅ.[64] Unfortunately, the quadrupole moment can only be measured for molecules that have no dipole moment. However, the influence of the hydroxyl substituent on the quadrupole moment of the aromatic ring can be estimated by considering the inductive effects of the substituent. Hydroxyl substituents are known to have both electron-donating (mesomeric) and electron-withdrawing (inductive) effects on the aromatic ring. However, the mesomeric effect is somewhat greater than the inductive effect resulting in a slight increase in the electron density of the aromatic π system. The mesomeric effect arises from one of the lone pairs of electrons on the O atom being partially delocalized over the aromatic ring as shown in the Lewis structures of phenol below.

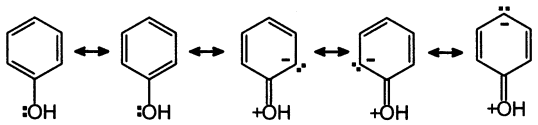

Because oxygen is fairly electronegative, the latter three resonance structures are much less favorable than the first two structures. Nevertheless, these later resonance structures do contribute to the overall stability of phenol. The delocalization of electron density into the ring results in the C−O bond taking on some double-bond character; the C−O bond distance in phenol is ∼0.05 Å shorter than it is in aliphatic alcohols such as methanol and ethanol. Therefore, the hydroxyl substituent results in a small increase in the quadrupole moment and therefore the strength of the cation−π interaction. The polarizability of benzene is estimated using the additivity method of Miller[40] to be 9.99 Å^3 and increases to 11.00 Å^3 for phenol. Therefore, the ion-induced dipole interaction should also result in slightly stronger binding to phenol than that observed for benzene. As discussed above, a cation−π interaction between an alkali metal cation and an aromatic ligand is expected to be largely electrostatic, arising from ion−dipole, ion−quadrupole, and ion-induced dipole interactions, but dominated by the ion−quadrupole interaction. All of these effects act in concert to increase the strength of the cation−π interaction in the phenol complexes. The increase in the cation−π BDEs to phenol, relative to those of benzene, varies between 0.2 and 17.4 kJ/mol for the mono-complexes and 0.9 and 10.3 for the bis-complexes. The enhancement is greatest for the Li^+ and Na^+ complexes and is quite small for the K^+, Rb^+, and Cs^+ complexes.

***σ*-Binding Versus Cation−*π* Complexes.** As discussed in the Theoretical Results section, σ-binding conformers are also found for these systems. The relative stabilities of the σ-binding versus cation−π complexes is such that at 298 K, the temperature of the reactant ions, the distribution of ions created in our source is probably a mixture of the σ-binding and cation−π complexes for all metal cations. The relative populations of the σ-binding complexes for the Li^+ systems is probably quite small. The small population of the σ-binding conformers that may be present in our beam would tend to lower the measured threshold for the CID of these complexes. However, this effect should be very small for the Li^+ systems as a result of the small population of the σ-binding conformers that might be present. The ground state of $K^+(C_6H_5OH)$ is also found to be the cation−π complex. However, it is only favored by 1.5 kJ/mol over the σ-binding complex, suggesting that at 298 K about 35% of the ions are likely to be the σ-binding conformers. In contrast, the calculations find that ground states of the $Na^+(C_6H_5OH)$ and $Rb^+(C_6H_5$-

OH) complexes are σ-conformers, by 0.6 and 1.1 kJ/mol, respectively. This suggests that at 298 K about 56 and 61% of the ions are likely to be the σ-binding conformers, respectively. The calculations find that the cation$-\pi$ and σ-binding conformers of $Cs^+(C_6H_5OH)$ to be degenerate. This suggests that both conformers are likely to be present in our experiments in roughly equal populations. Because the binding energies of the σ-binding and cation$-\pi$ complexes are very nearly equal for all but the Li^+ systems, the affect on the threshold determination should be almost negligible.

The σ-binding conformers are nearly "2-D structures" and would be expected to have a smaller cross section than the analogous cation$-\pi$ complexes. Thus, the smaller cross sections observed for the Rb^+ and Cs^+ complexes as compared with the other alkali metal cations suggests that indeed these ion beams are probably composed of a fair fraction of σ-binding conformers. The fact that the cross sections are larger to Na^+ and K^+ even though these ions bind phenol more strongly suggests that the σ-binding conformers produced in our source may not be as abundant as the calculations suggest in these systems. Overall, our results suggest that the near degeneracy of the cation$-\pi$ and σ-binding complexes would make it possible for the complexes of phenol to Na^+, K^+, Rb^+ and Cs^+ to take on either conformation dependent upon the local environment. Such flexibility of alkali metal cation binding to phenol, or more biologically relevant tyrosine, may prove functionally important during conformational changes of proteins that occur during various biological processes.

Comparison with Other $M^+(C_6H_5OH)$ Complexes. As mentioned in the Introduction, studies of cation$-\pi$ interactions of other metal cations with phenol have been reported. Ryzhov and Dunbar[27] examined the interactions of Mg^+, Al^+, Cr^+, and Fe^+ with phenol both experimentally and theoretically. Using radiative associative methods, they measured BDEs of Mg^+, Al^+, and Cr^+ to phenol of 160, 157, and 206 kJ/mol, respectively. In Fe^+, they were only able to determine a lower limit for this BDE of 239 kJ/mol. In their analysis they assumed that both Mg^+ and Al^+ took on σ-binding conformations rather than cation$-\pi$ conformations as suggested by their theoretical calculations. The calculated BDEs of the Na^+, Mg^+, Al^+, Cr^+, and Fe^+ (^4F, d^7) cation$-\pi$ complexes to phenol are 99, 131, 127, 157, and 263 kJ/mol (including BSSE and ZPE corrections), respectively. Calculations were also performed for Fe^+ in its ground-state electronic configuration (^6D, s^1d^6), which binds phenol much less strongly, by 82 kJ/mol (excluding BSSE and ZPE corrections). The BDEs of the corresponding σ-binding complexes are calculated to be 101, 138, 129, 150, and 193 kJ/mol (including BSSE and ZPE corrections), respectively. Thus, theory suggests that the σ-binding conformations are favored over the cation$-\pi$ complexes for Na^+, Mg^+, and Al^+; whereas the converse is true for Cr^+ and Fe^+. On the basis of experimental and theoretical results from their work along with literature values for benzene, Ryzhov and Dunbar provided "best-estimate BDEs" to Na^+ and K^+ in addition to the Mg^+, Al^+, Cr^+, and Fe^+ metal cations. Their "best-estimate" values for the BDEs of Na^+, K^+, Mg^+, Al^+, Cr^+, and Fe^+ to phenol are 117 ± 13, 84 ± 13, 155 ± 17, 159 ± 17, 180 ± 17, and 251 ± 25 kJ/mol, respectively. The "best-estimate" values for Na^+ and K^+ are $\sim$15% greater than the values measured here. The binding in the complexes to metal cations other than the alkalis is much stronger as a result of the contribution to the binding made by the valence electrons. This enhanced binding is much larger for the transition metal cations than for Mg^+ and Al^+, primarily because the transition metal cations are much smaller allowing the phenol ligand to approach the metal cation more closely. Schroeter et al.[38] also investigated complexes of phenol with Cr^+, Fe^+, and Co^+ using Cook's kinetic method. They measured BDEs of Cr^+, Fe^+, and Co^+ to phenol of 172 ± 11, 209 ± 11, and 255 ± 11 kJ/mol, respectively. Their value for Cr^+ is within experimental error of that measured by Ryzhov and Dunbar. However, the value they determine for Fe^+ is significantly below the "best-estimate", and even below the lower limit reported by Ryzhov and Dunbar possibly indicating that a different electronic state of $Fe^+(C_6H_5OH)$ was accessed in their experiments. The values Schroeter et al. found for the $M^+(C_6H_5OH)$ complexes differ only slightly from the values measured for the analogous $M^+(C_6H_6)$ complexes. Their results suggest that Cr^+ and Fe^+ bind phenol more strongly than benzene by $\sim$2 kJ/mol, whereas Co^+ binds phenol less strongly than benzene by 0.4 kJ/mol. They concluded that the similarity in the strength of binding to phenol and benzene results from the electronegativity of the hydroxyl group being canceled by the interaction of the aromatic system with the lone pairs of the oxygen atom. In contrast Ryzhov and Dunbar find that the binding to phenol is stronger than to benzene for all of the metal cations they examined except Na^+, which binds benzene and phenol about equally as strongly, in accord with the present results.

Conclusions

The kinetic energy dependence of the collision-induced dissociation of $M^+(C_6H_5OH)_x$ complexes ($M^+ = Li^+$, Na^+, K^+, Rb^+, and Cs^+, $x =$ 1and 2), with Xe is examined in a guided ion beam tandem mass spectrometer. The dominant dissociation pathway observed for all complexes is loss of an intact phenol ligand. Thresholds for these dissociation reactions are determined after careful consideration of the effects of reactant internal energy, multiple collisions with Xe, and the lifetime of the ionic reactants. The molecular parameters needed for the analysis of experimental data as well as structures and theoretical estimates of the BDEs for the $M^+(C_6H_5OH)_x$ complexes are obtained from theoretical calculations performed at the MP2-(full)/6-311+G(2d,2p)//B3LYP/6-31G(d) level. The absolute M^+-(C_6H_5OH) and (C_6H_5OH)M^+-(C_6H_5OH) BDEs are observed to decrease monotonically as the size of the alkali metal cation increases from Li^+ to Cs^+. Similarly, the difference in the BDEs of the mono- and bis-complexes are also observed to decrease monotonically with the size of the alkali metal cation. These trends are explained in terms of the electrostatic nature of the bonding in the $M^+(C_6H_5OH)_x$ complexes and the changes in magnitude of the ligand$-$ligand interactions in the $M^+(C_6H_5OH)_2$ complexes, respectively. The agreement between experiment and theory is very good when full electron correlation is included, for Li^+, Na^+, and K^+. However, significant deviations are observed for the mono-ligated $Li^+(C_6H_5OH)$ complex. When effective core potentials are used, for Rb^+ and Cs^+, theory is found to underestimate the strength of the binding. An interesting observation is that the σ-binding and cation$-\pi$ complexes of Na^+, K^+, Rb^+, and Cs^+ are calculated to be of very similar stability. Therefore, a mixture of these two conformers is probably accessed in our experiments. Because of the very small differences in the binding energies of the σ-binding and cation$-\pi$ complexes of these systems, the effects on our threshold measurements should be minimal. Comparisons made with other alkali metal cation$-\pi$ complexes previously studied reveal that the most important effects that substituents have on the strength of cation$-\pi$ interactions arise from their influence on the π electron density of the aromatic ring and the increase

they produce in the polarizability of the ligand. Overall, the hydroxyl substituent leads to a small increase in the strength of the cation−π interaction, in both the mono- and bis-complexes, to all of the alkali metal cations in accord with its influence on the quadrupole moment and polarizability.

Acknowledgment. This work was supported by National Science Foundation Grant 0138504.

Supporting Information Available: Tables of vibrational frequencies, average vibrational energies, and rotational constants, and B3LYP/6-31G* geometry-optimized structures for neutral C_6H_5OH and the $M^+(C_6H_5OH)_x$ complexes. Figures showing cross sections for the collision-induced dissociation of $M^+(C_6H_5OH)_x$ complexes with Xe as well as empirical fits to the primary product channels (where $M^+ = Li^+$, K^+, Rb^+, and Cs^+) (PDF). This material is available free of charge via the Internet at http://pubs.acs.org.

References and Notes

(1) Ma, J. C.; Dougherty, D. A. *Chem. Rev.* **1997**, *97*, 1303.
(2) Dougherty, D. A. *Science* **1996**, *271*, 163.
(3) DeVos, A. M.; Ultsch, M.; Kossiakoff, A. A. *Science* **1992**, *255*, 306.
(4) Karlin, A. *Curr. Opin. Neurobiol.* **1993**, *3*, 299.
(5) Raves, M. L.; Harel, M.; Pang, Y. P.; Silman, I.; Kozikowski, A. P.; Sussman, J. L. *Nat. Struct. Biol.* **1997**, *4*, 57.
(6) Stauffer, D. A.; Karlin, A. *Biochemistry* **1994**, *33*, 6840.
(7) Mitchell, J. B.; Nandi, C. L.; McDonald, I. K.; Thornton, J. M.; Price, S. L. *J. Mol. Biol.* **1994**, *239*, 315.
(8) Zhong, W.; Gallivan, J. P.; Zhang, Y.; Li, L.; Lester, H. A.; Dougherty, D. A. *Proc. Natl. Acad. Sci. U.S.A.* **1998**, *95*, 12088.
(9) Donini, O.; Weaver, D. F. *J. Comput. Chem.* **1998**, *19*, 1515.
(10) Heginbotham, L.; Lu, Z.; Abramson, T.; MacKinnon, R. *Biophys. J.* **1994**, *66*, 1061.
(11) Nakamura, R. L.; Anderson, J. A.; Gaber, R. F. *J. Biol. Chem.* **1997**, *272*, 1011.
(12) Heginbotham, L.; MacKinnon, R. *Neuron* **1992**, *8*, 483.
(13) MacKinnon, R.; Yellen, G. *Science* **1990**, *250*, 276.
(14) Kavanaugh, M. P.; Varnum, M. D.; Osborne, P. B.; Christle, M. J.; Busch, A. E.; Adelman, J. P.; North, R. A. *J. Biol. Chem.* **1991**, *266*, 7583.
(15) Kavanaugh, M. P.; Hurst, R. S.; Yakel, J.; Varnum, M. D.; Adelman, J. P.; North, R. A. *Neuron* **1992**, *8*, 493.
(16) Satin, J.; Kyle, J. W.; Chen, M.; Bell, P.; Cribs, L. L.; Fozzard, H. A.; Rogart, R. B. *Science* **1992**, *256*, 1202.
(17) Lippard, S. J.; Berg, J. M. *Principles of Bioinorganic Chemistry*; University Science Books: Mill Valley, CA, 1994.
(18) Gokel, G. W.; De Wall, S. L.; Meadows, E. S. *Eur. J. Org. Chem.* **2000**, 2967.
(19) Sunner, J.; Nishizawa, K.; Kebarle, P. *J. Phys. Chem.* **1981**, *85*, 1814.
(20) Woodin, R. L.; Beauchamp, J. L. *J. Am. Chem. Soc.* **1978**, *100*, 501.
(21) Taft, R. W.; Anvia, F.; Gal, J.-F.; Walsh, S.; Capon, M.; Holmes, M. C.; Hosn, K.; Oloumi, G.; Vasanwala, R.; Yazdani, S. *Pure Appl. Chem.* **1990**, *62*, 17.
(22) Guo, B. C.; Purnell, J. W.; Castleman, A. W., Jr. *Chem. Phys. Lett.* **1990**, *168*, 155.
(23) Armentrout, P. B.; Rodgers, M. T. *J. Phys. Chem. A* **2000**, *104*, 2238.
(24) Amicangelo, J. C.; Armentrout, P. B. *J. Phys. Chem. A* **2000**, *104*, 11420.
(25) Gapeev, A.; Yang, C.-Y.; Klippenstein, S. J.; Dunbar, R. C. *J. Phys. Chem. A* **2000**, *104*, 3246.
(26) Huang, H.; Rodgers, M. T. *J. Phys. Chem. A* **2002**, *106*, 4277.
(27) Ryzhov, V.; Dunbar, R. C. *J. Am. Chem. Soc.* **1999**, *121*, 2259.
(28) Amunugama, R.; Rodgers, M. T. *J. Phys. Chem. A* **2002**, *106*, 5529.
(29) Ryzhov, V.; Dunbar, R. C.; Cerda, B.; Wesdemiotis, C. *J. Am. Soc. Mass Spectrom.* **2000**, *11*, 1037.
(30) Gapeev, A.; Dunbar, R. C. *J. Am. Chem. Soc.* **2001**, *123*, 8360.
(31) Amunugama, R.; Rodgers, M. T. *J. Phys. Chem. A* **2002**, *106*, 9092. Date August 13, 2002.
(32) Amunugama, R.; Rodgers, M. T. *Int. J. Mass Spectrom.*, in press.
(33) Feller, D.; Dixon, D. A.; Nicholas, J. B. *J. Phys. Chem. A* **2000**, *104*, 11414.
(34) Tsuzuki, S.; Yoshida, M.; Uchimaru, T.; Mikami, M. *J. Phys. Chem. A* **2001**, *105*, 769.
(35) Mecozzi, S.; West, A. P. Jr.; Dougherty, D. A. *J. Am. Chem. Soc.* **1996**, *118*, 2307.
(36) McMahon, T. B.; Ohanessian, G. *Chem. Eur. J.* **2000**, *6*, 2931.
(37) Hoyau, S.; Norrman, K.; McMahon, T. B.; Ohanessian, G. *J. Am. Chem. Soc.* **1999**, *121*, 8864.
(38) Schroeter, K.; Wesendrup, R.; Schwarz, H. *Eur. J. Org. Chem.* **1998**, *565*, 5.
(39) *Handbook of Chemistry and Physics*; Weast, R. C., Astle, M. J., Eds. CRC Press: Boca Raton, FL, 1982; p. E−61.
(40) Miller, K. J. *J. Am. Chem. Soc.* **1990**, *112*, 8533.
(41) Rodgers, M. T.; Ervin, K. M.; Armentrout, P. B. *J. Chem. Phys.* **1997**, *106*, 4499.
(42) Rodgers, M. T. *J. Phys. Chem. A* **2001**, *105*, 2374.
(43) Teloy, E.; Gerlich, D. *Chem. Phys.* **1974**, *4*, 417. Gerlich, D. Diplomarbeit, University of Freiburg, Federal Republic of Germany, 1971. Gerlich, D. *Adv. Chem. Phys*. **1992**, *82*, 1.
(44) Ervin, K. M.; Armentrout, P. B. *J. Chem. Phys*. **1985**, *83*, 166.
(45) Dalleska, N. F.; Honma, K.; Sunderlin, L. S.; Armentrout, P. B. *J. Am. Chem. Soc.* **1994**, *116*, 3519.
(46) Beyer, T. S.; Swinehart, D. F. *Commun. ACM* **1973**, *16*, 379. Stein, S. E.; Rabinovitch, B. S. *J. Chem. Phys.* **1973**, *58*, 2438; *Chem. Phys. Lett.* **1977**, *49*, 1883.
(47) Pople, J. A.; Schlegel, H. B.; Ragavachari, K.; deFrees, D. J.; Binkley, J. F.; Frisch, M. J.; Whitesides, R. F.; Hout, R. F.; Hehre, W. J. *Int. J. Quantum Chem. Symp.* **1981**, *15*, 269. deFrees, D. J.; McLean, A. D. *J. Chem. Phys.* **1985**, *82*, 333.
(48) Khan, F. A.; Clemmer, D. C.; Schultz, R. H.; Armentrout, P. B. *J. Phys. Chem*. **1993**, *97*, 7978.
(49) Chesnavich, W. J.; Bowers, M. T. *J. Phys. Chem.* **1979**, *83*, 900.
(50) See, for example, Figure 1 in Dalleska, N. F.; Honma, K.; Armentrout, P. B. *J. Am. Chem. Soc.* **1993**, *115*, 12125.
(51) Armentrout, P. B.; Simons, J. *J. Am. Chem. Soc.* **1992**, *114*, 8627.
(52) Frisch, M. J.; Trucks, G. W.; Schlegel, H. B.; Scuseria, G. E.; Robb, M. A.; Cheeseman, J. R.; Zakrzewski, V. G.; Montgomery, J. A., Jr.; Stratmann, R. E.; Burant, J. C.; Dapprich, S.; Millam, J. M.; Daniels, A. D.; Kudin, K. N.; Strain, M. C.; Farkas, O.; Tomasi, J.; Barone, V.; Cossi, M.; Cammi, R.; Mennucci, B.; Pomelli, C.; Adamo, C.; Clifford, S.; Ochterski, J.; Petersson, G. A.; Ayala, P. Y.; Cui, Q.; Morokuma, K.; Malick, D. K.; Rabuck, A. D.; Raghavachari, K.; Foresman, J. B.; Cioslowski, J.; Ortiz, J. V.; Stefanov, B. B.; Liu, G.; Liashenko, A.; Piskorz, P.; Komaromi, I.; Gomperts, R.; Martin, R. L.; Fox, D. J.; Keith, T.; Al-Laham, M. A.; Peng, C. Y.; Nanayakkara, A.; Gonzalez, C. Challacombe, M.; Gill, P. M. W.; Johnson, B.; Chen, W. Wong, M. W.; Andres, J. L.; Gonzales, C.; Head-Gordon, M.; Replogle, E. S.; Pople, J. A. *Gaussian 98*, Revision A.11; Gaussian, Inc.: Pittsburgh, PA, 1998.
(53) Becke, A. D. *J. Chem. Phys.* **1993**, *98*, 5648.
(54) Lee, C.; Yang, W.; Parr, R. G. *Phys. Rev. B* **1988**, *37*, 785.
(55) Hay, P. J.; Wadt, W. R. *J. Chem. Phys.* **1985**, *82*, 299.
(56) Glendening, E. D.; Feller, D.; Thompson, M. A. *J. Am. Chem. Soc.* **1994**, *116*, 10657.
(57) Walter, D.; Armentrout, P. B. *J. Am. Chem. Soc*. **1998**, *120*, 3176.
(58) Foresman, J. B.; Frisch, M. J. *Exploring Chemistry with Electronic Structure Methods*, 2nd ed.; Gaussian: Pittsburgh, 1996; p 64.
(59) Boys, S. F.; Bernardi, R. *Mol. Phys.* **1979**, *19*, 553.
(60) Van Duijneveldt, F. B.; van Duijneveldt-van de Rijt, J. G. C. M.; van Lenthe, J. H. *Chem. Rev.* **1994**, *94*, 1873.
(61) Lifshitz, C. *Adv. Mass Spectrom.* **1989**, *11*, 113.
(62) The metal ring-centroid distance is defined as the distance from the metal cation to the central point within the aromatic ring that is in the plane of the carbon atoms.
(63) Wilson, R. G.; Brewer, G. R. *Ion Beams: With Applications to Ion Implantation*; Wiley: New York, 1973; pp 118−124.
(64) Williams, J. H. *Acc. Chem. Res*. **1993**, *26*, 593.